Int J Clin Exp Med 2019;12(8):10075-10083
www.ijcem.com /ISSN:1940-5901/IJCEM0093855

Original Article

Tanshindiol C inhibits proliferation and induces apoptosis in non-small cell lung cancer by modulating miR-491-3p expression

Dan Gu*, Hui-Wen Weng*, Bi-Yu Xu

*Department of Traditional Chinese Medicine, The First Affiliated Hospital of Sun Yat-sen University, Guangzhou 510080, China. *Equal contributors.*

Received March 14, 2019; Accepted June 6, 2019; Epub August 15, 2019; Published August 30, 2019

Abstract: Background: Tanshindiol C (TanC) has been validated to repress proliferation in several cancer cell types. However, the underlying molecular mechanism of TanC on non-small cell lung cancer (NSCLC) cell proliferation and apoptosis is unclear. The aim of the present study was to explore whether microRNAs (miRNAs) and downstream target were involved in TanC-induced NSCLC cell death *in vitro*. Methods: miRNAs expression profiling was analyzed in A549 cells with or without TanC treatment using miRNAs microarray. Cell viability and apoptosis were detected using CCK8 and Annexin V-fluorescein isothiocyanate/propidium iodide (Annexinv-FITC) double staining, respectively. Bioinformatics algorithms and luciferase reporter assay were performed to verify c-MYC as a direct target of miR-491-3p. Results: TanC showed an anti-proliferative and pro-apoptotic activity in A549 and H358 cells. We also found that an increase in miR-491-3p and a decrease in c-MYC expression levels were observed in TanC-stimulated A549 and H358 cells. c-MYC was a direct target of miR-491-3p, and overexpression of miR-491-3p repressed c-MYC protein expression by directly binding with the 3'-UTR of c-MYC. miR-491-3p mimics induced growth inhibition and apoptosis were abolished by the overexpression of c-MYC in A549 and H358 cells. Conclusion: TanC had an effective ability to inhibit proliferation and induce apoptosis in NSCLC cells, and the underlying mechanism was mediated, at least partially, by regulating miR-491-3p/c-MYC signaling pathway.

Keywords: Non-small cell lung cancer, tanshindiol C, miR-491-3p, c-MYC, apoptosis

Introduction

Lung cancer is one of the most common malignant tumors and the leading cause of cancer-related death worldwide, accounting for approximately 13% of total cancer cases [1]. Cancer statistics in China estimates that 733,300 cases is newly diagnosed and 610,200 deaths occur in 2015 [2]. In addition, about 85% of lung cancer cases are diagnosed with non-small cell lung cancer (NSCLC), with a 5-year survival rate less than 20% [3]. Although important advancements of pharmacotherapy have been achieved in the treatment of NSCLC, the overall survival rates for NSCLC remain low, particularly in advanced and metastatic disease [4]. Therefore, continued research of new treatment strategies is significant for improving outcomes in NSCLC patients.

Tanshindiol C (TanC) is the major active ingredient of *Salvia miltiorrhiza* Bge, which is a traditional Chinese medicine for the prevention and treatment of several diseases, including atherosclerosis [5], type 2 diabetes mellitus [6] and immune disorders [7]. Recently, several active ingredients, such as tanshinone I [8], tanshinone IIA [9, 10], cryptotanshinone [11, 12] salvianolic acid A and B [13, 14], of *Salvia miltiorrhiza* Bge have been validated to exhibit an antineoplastic activity in various types of human cancer. However, the roles and underlying molecular mechanisms of TanC on proliferation and apoptosis of human NSCLC cells are still unclear.

MicroRNAs (miRNAs/miRs) as a class of non-coding RNAs (approximately 22 nucleotides) perform a primarily function to repress tran-

scription or translation of target genes by binding with the 3'-untranslated region (3'-UTR) of target messenger RNA (mRNA), which results in mRNA cleavage and degradation or translational repression [15]. Previous studies have been identified that numerous miRNAs are reported in a variety of physiological and pathological processes, including tumorigenesis [16, 17]. Accumulating evidence reveals that deregulation of miRNAs contributes to the initiation and progression of NSCLC [18, 19]. Our present study aimed to investigate miRNAs expression profiling in TanC-treated NSCLC cells using miRNAs microarray assays, and the results demonstrated that miR-491-3p was significantly upregulated in TanC-treated NSCLC cells. Subsequently, we validated the expression of miR-491-3p in NSCLC cells using RT-qPCR analysis. Furthermore, in vitro experiments were performed to detect the roles of miR-491-3p on proliferation and apoptosis via transfection with miR-491-3p mimics or inhibitors into NSCLC cells.

Materials and methods

Cell culture

Human normal 16HBE cells (Cell Bank of China Academy of Sciences, Shanghai, China) and four kinds of NSCLC cells (ATCC, American Type Culture Collection, Manassas, VA, USA), A549, H358, SK-MES-1 and H1299, were cultured in Dulbecco's modified Eagle's medium (DMEM; Invitrogen, Carlsbad, CA, USA) with 10% fetal bovine serum (Thermo Scientific HyClone, Beijing, China), 100 U/ml penicillin and 100 mg/ml streptomycin in a humidified incubator (Thermo Fisher Scientific, Inc., Waltham, MA, USA), 5% CO_2, 95% air atmosphere.

CCK8 assay

NSCLC cells (1×10^4) were seeded in the 96-well plate and cultured with CCK8 solution (10 μL, Beyotime Institute of Biotechnology, Haimen, China). A spectrophotometer (Thermo Scientific, Rockford, IL, USA) was used to measure the absorbance at 450 nm.

miRNAs microarray analysis

Differentially expressed miRNAs in A549 cells with or without TanC treatment were analyzed using the SurePrint G3 Human miRNA Microarray (8x60K, Agilent Technologies, Santa Clara, CA, USA) according to previously described method [20].

Reverse transcription-quantitative polymerase chain reaction (RT-qPCR)

Total RNA was isolated using RNAiso (Takara, Dalian, China). TaqMan® RT kit (Applied Biosystems; Thermo Fisher Scientific, Inc.) and TaqMan® MicroRNA assay (Applied Biosystems; Thermo Fisher Scientific, Inc.) were used to measure the expression levels of miRNAs using Applied Biosystems 7300 Real-Time PCR System (Thermo Fisher Scientific, Inc.) and normalized to the internal control U6. miRNAs expression levels were calculated using the $2^{-\Delta\Delta Cq}$ method [21]. In addition, TaqMan Universal PCR Master Mix (Thermo Fisher Scientific, Inc.) was used to measure the expression levels of c-MYC using Applied Biosystems 7300 Real-Time PCR System. c-MYC mRNA expression levels were calculated using the $2^{-\Delta\Delta Cq}$ method [21] and normalized to glyceraldehyde 3-phosphate dehydrogenase (GAPDH). The primers were shown as follows: c-MYC: forward primer 5'-CCTGGTGCTCCATGAGGAGAC-3' and reverse primer 5'-CAGACTCTGACCTTTTGCCAGG-3'; GAPDH: forward primer 5'-TTGGCCAGGGGTGCTAAG-3' and reverse primer 5'-AGCCAAAAGGGTCATCATCTC-3'.

Annexinv-FITC double staining for apoptosis

Cell apoptosis was analyzed using Annexin V-FITC/PI double staining kit (Invitrogen, Carlsbad, Calif, USA). Flow cytometry (FACScan, BD Biosciences, San Jose, CA, USA) and CELL Quest 3.0 software (BD Biosciences) were used to calculate the apoptotic cell proportion in A549 and H358 cells.

miRNA and plasmid transfection

miR-control (miR-Con; 5'-CUUGUGGUAAUGUCCUGUUAGU-3'), miR-491-3p mimics (5'-CUUAUGCAAAGAUUCCCUUCUA-3') and inhibitors (5'-UAGAAGGGAAUCUUUGCAUAAG-3') were synthesized by Guangzhou RiboBio Co., Ltd. (Guangzhou, China). A mammalian expression plasmid designed to specially express the full-length open reading frame of human c-MYC without 3'-UTR was purchased from GeneCopoeia, Inc. (Rockville, MD, USA). An empty plasmid served as the negative control. miR-Con, miR-491-3p mimics, inhibitors, vector-Con and vector-c-MYC were transfected into A549 and H358

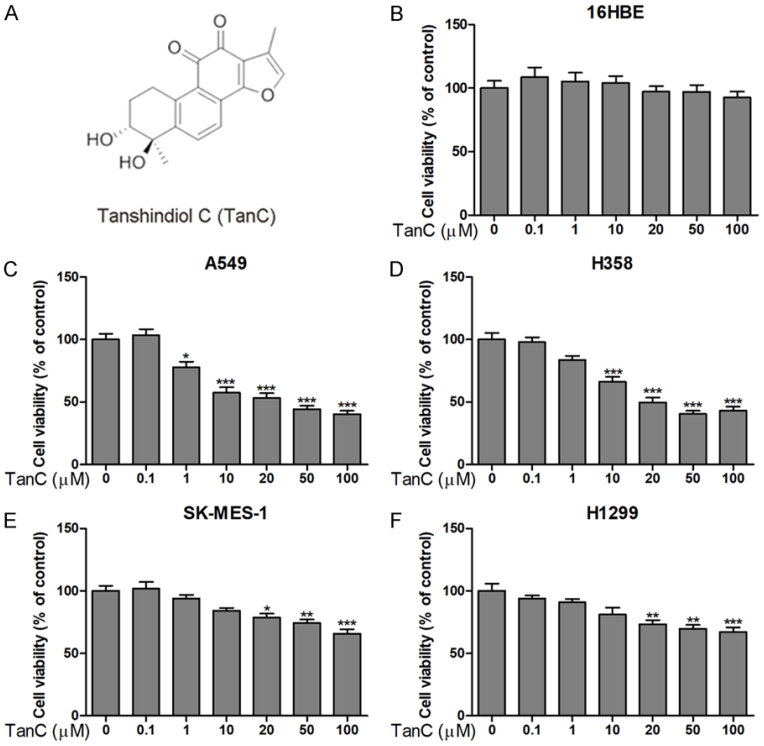

Figure 1. TanC exhibited the ability to induce growth inhibition in NSCLC cells. The molecular structure of TanC (molecular weight: 312.3; A). The cytotoxicity of TanC was validated in human normal 16HBE cells, and the results demonstrated that TanC treatment had no obvious influence on cell viability when cultured for 48 h (B). CCK8 assays were used to detect the cell viability of A549 (C), H358 (D), SK-MES-1 (E) and H1299 (F) cells with or without TanC treatment for 48 h. $^{*}P < 0.05$, $^{**}P < 0.01$, $^{***}P < 0.001$ compared with the control group.

cells using Lipofectamine 2000 for 48 h at 37°C, according to the manufacturer's protocols.

Luciferase reporter assay

The wild-type (WT) and mutant-type (MUT) 3'-UTR of c-MYC were inserted into the multiple cloning sites of the luciferase expressing pMIR-REPORT vector (Ambion; Thermo Fisher Scientific, Inc.), which were co-transfected with miR-Con, miR-491-3p mimics or inhibitors into A549 and H358 cells. The luciferase activity was measured using a luciferase reporter assay kit (Promega, Madison, WI, USA).

Western blotting

Total protein in A549 and H358 cells was extracted using radio immunoprecipitation assay buffer (Beyotime Institute of Biotechnology, Haimen, China). Western blotting analysis was performed as described previously [22]. The primary antibody of c-MYC (cat.#: sc-4084; dilution: 1:1,000; Santa Cruz Biotechnology, Santa Cruz, CA, USA) and horseradish peroxidase-conjugated secondary antibody were purchased from Santa Cruz Biotechnology (cat.#: sc-516102; dilution: 1:10,000; Santa Cruz Biotechnology, Santa Cruz, CA, USA). Protein bands were visualized using chemiluminescence (Thermo Fisher Scientific, Inc.). Signals were analyzed with Quantity One® software version 4.5 (Bio Rad Laboratories, Inc., Hercules, CA, USA). β-actin (cat.#: sc-130301; dilution: 1:2,000; Santa Cruz Biotechnology, Santa Cruz, CA, USA) signals were used to correct for unequal loading.

Statistical analysis

All data were showed as mean ± standard error of mean. PRISM version 7.0 (GraphPad Software, Inc., La Jolla, CA, USA) was used to perform the statistical analysis. Inter-group differences were analyzed by one-way analysis of variance, followed by a post hoc Tukey test for multiple comparisons. $P < 0.05$ was considered as statistical significance.

Results

TanC exhibited the ability to induce growth inhibition in NSCLC cells

To explore the antineoplastic activity of TanC *in vitro*, we investigated the cytotoxicity of TanC on human normal 16HBE cells, and the results demonstrated that TanC treatment had no obvious influence on cell viability when cultured for 48 h with the concentration in the range of 0 μM to 100 μM (**Figure 1B**). Next, the four kinds of NSCLC cells, including A549, H358, SK-MES-1 and H1299, were exposed to TanC for 48 h, the experimental measurements showed that TanC administration led to cell growth retardation in NSCLC cell lines in a dose-dependent manner (**Figure 1C-F**). Collectively, these

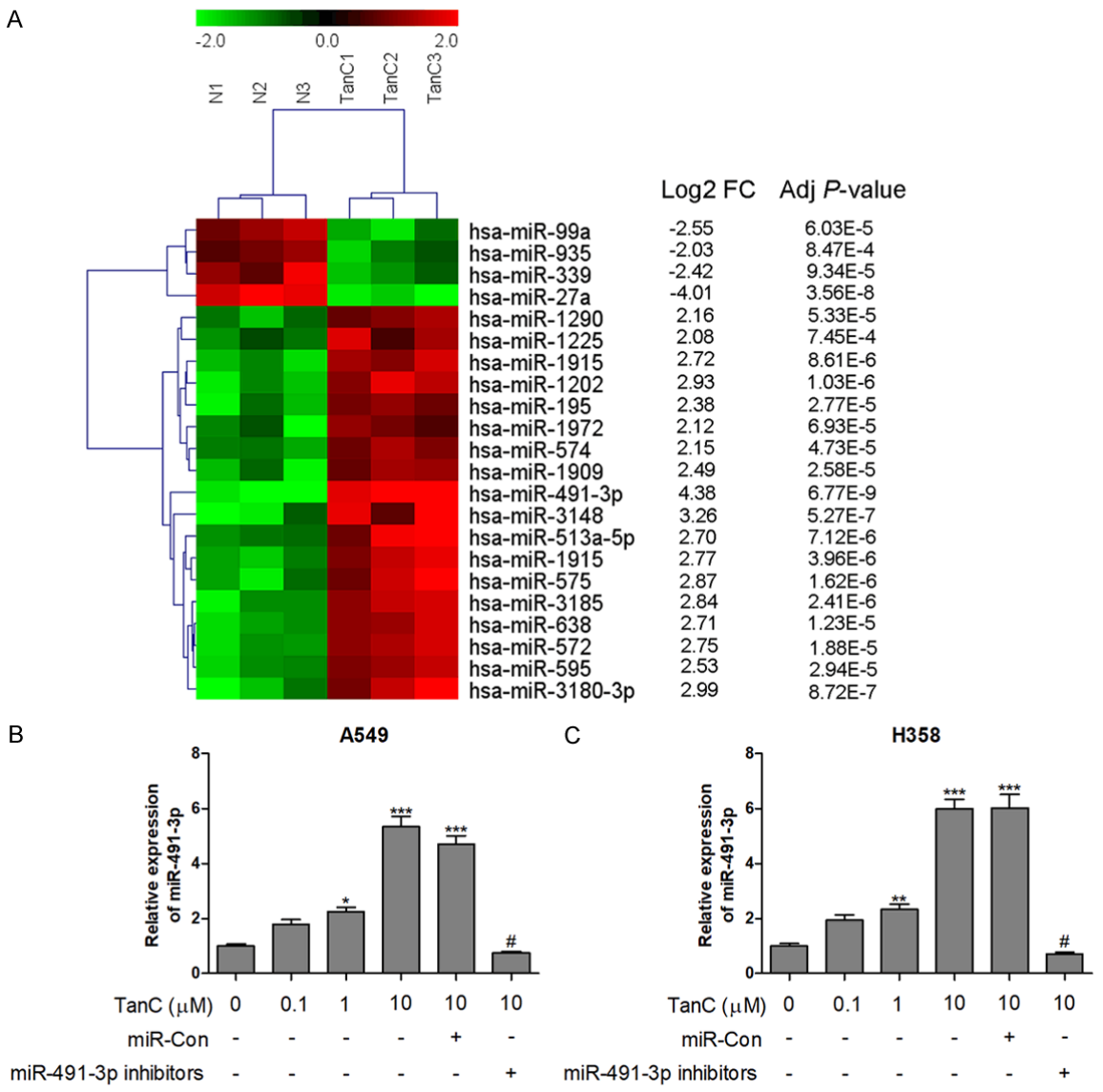

Figure 2. miRNAs expression profiling in TanC-treated A549 cells. Microarray and hierarchical cluster analysis were performed using the multiple experiment viewer 4.7.1 software, and 22 differentially expressed miRNAs in TanC-stimulated A549 cells were selected out according to |Log2 fold change| ≥ 2 and FDR ≤ 0.001 (A). After transfection with miR-491-3p inhibitors into TanC-treated A549 and H358 cells, the expression levels of miR-491-3p were measured by RT-qPCR (B and C). $^{*}P < 0.05$, $^{**}P < 0.01$, $^{***}P < 0.001$ compared with the control group; $^{\#}P < 0.05$ compared with TanC (10 μM) treatment group.

data indicated that TanC had the ability to prevent NSCLC cell proliferation *in vitro*.

miRNAs expression profiling in TanC-treated A549 cells

To determine the molecular mechanism underlying TanC-induced growth inhibition in NSCLC cells, we utilized miRNAs microarray to analyze miRNAs expression profiling in TanC-treated A549 cells. Based on |Log2 fold change| ≥ 2 and FDR ≤ 0.001, 22 miRNAs were significantly differentially expressed in TanC-stimulated A549 cells compared with that in the control group. Among these miRNAs, 4 miRNA were down-regulated and 18 miRNAs were up-regulated in TanC-stimulated A549 cells (**Figure 2A**). In addition, we observed that the expression levels of miR-491-3p were higher than other miRNAs in response to TanC stimulation. Therefore, we focused on miR-491-3p in our further study. To validate the regulation function of TanC on miR-491-3p expression, RT-qPCR was performed to measure miR-491-3p

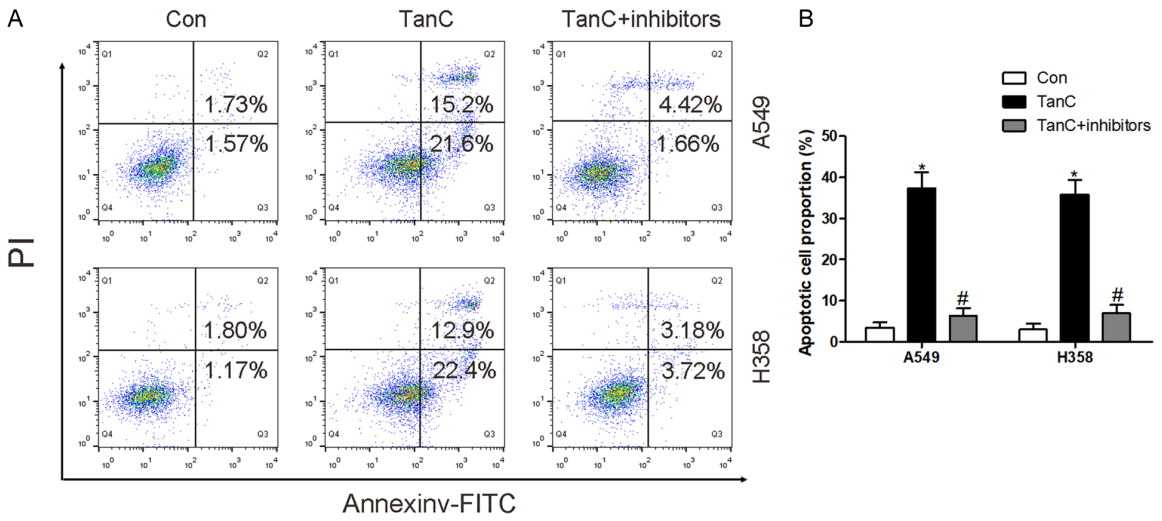

Figure 3. miR-491-3p inhibitors reversed the effects of TanC on cell apoptosis. After transfection with miR-491-3p inhibitors into TanC-treated A549 and H358 cells, cell was detected using Annexinv-FITC double staining with flow cytometry (A and B). $^{*}P < 0.05$ compared with the control group; $^{\#}P < 0.05$ compared with TanC (10 μM) treatment group.

expression in TanC-stimulated A549 and H358 cells, and an up-regulation of miR-491-3p expression was observed in A549 and H358 cells after exposure to TanC (**Figure 2B** and **2C**). Interestingly, transfection with miR-491-3p inhibitors into A549 and H358 cells blocked TanC-induced up-regulation of miR-491-3p expression (**Figure 2B** and **2C**). Taken together, these findings suggested that miR-491-3p, as a post-transcriptional regulator, might be involved in TanC-induced NSCLC cell growth inhibition.

Furthermore, we examined cell apoptosis in TanC-treated NSCLC cell. Annexinv-FITC double staining assays revealed that the apoptotic cell proportion was markedly increased in TanC-treated A549 and H358 cells as compared to the control group. Moreover, miR-491-3p inhibitors had been shown to attenuate the effects of TanC on cell apoptosis (**Figure 3A** and **3B**). These data indicated that TanC-induced NSCLC cell growth inhibition and apoptosis might be associated with the up-regulation of miR-491-3p expression in A549 and H358 cells.

miR-491-3p negatively regulated c-MYC by directly binding to its 3'-UTR

To further investigate the potential target of miR-491-3p, bioinformatics algorithm was executed by Targetscan (www.targetscan.org) to predict the downstream target of miR-491-3p. We found that the 3'-UTR of c-MYC could bind to miR-491-3p with the high score, and the analogous complementary pairing domain (**Figure 4A**). Thus, a luciferase reporter assay was conducted to confirm whether c-MYC was a direct target of miR-491-3p. The luciferase activity was significantly reduced in A549 and H358 cells co-transfected with WT 3'-UTR of c-MYC and miR-491-3p mimics, while the luciferase activity was significantly increased in A549 and H358 cells co-transfected with WT 3'-UTR of c-MYC and miR-491-3p inhibitors (**Figure 4B**). However, the luciferase activity was not influenced by miR-491-3p mimics or inhibitors in A549 and H358 cells containing Mut 3'-UTR of c-MYC (**Figure 4B**). Western blotting experiments showed that the negative regulatory effect of miR-491-3p mimics (**Figure 4C**) and TanC (**Figure 4D**) on c-MYC protein expression was observed in A549 and H358 cells.

Overexpressed c-MYC rescued the miR-491-3p-mediated effects

Base on the above results, we found that miR-491-3p and c-MYC might play the reciprocal roles in the progression of NSCLC. We also found that the expression of miR-491-3p was dramatically decreased, and c-MYC was markedly increased in NSCLC cell lines compared with human normal 16HBE cells (**Figure 5A**). To

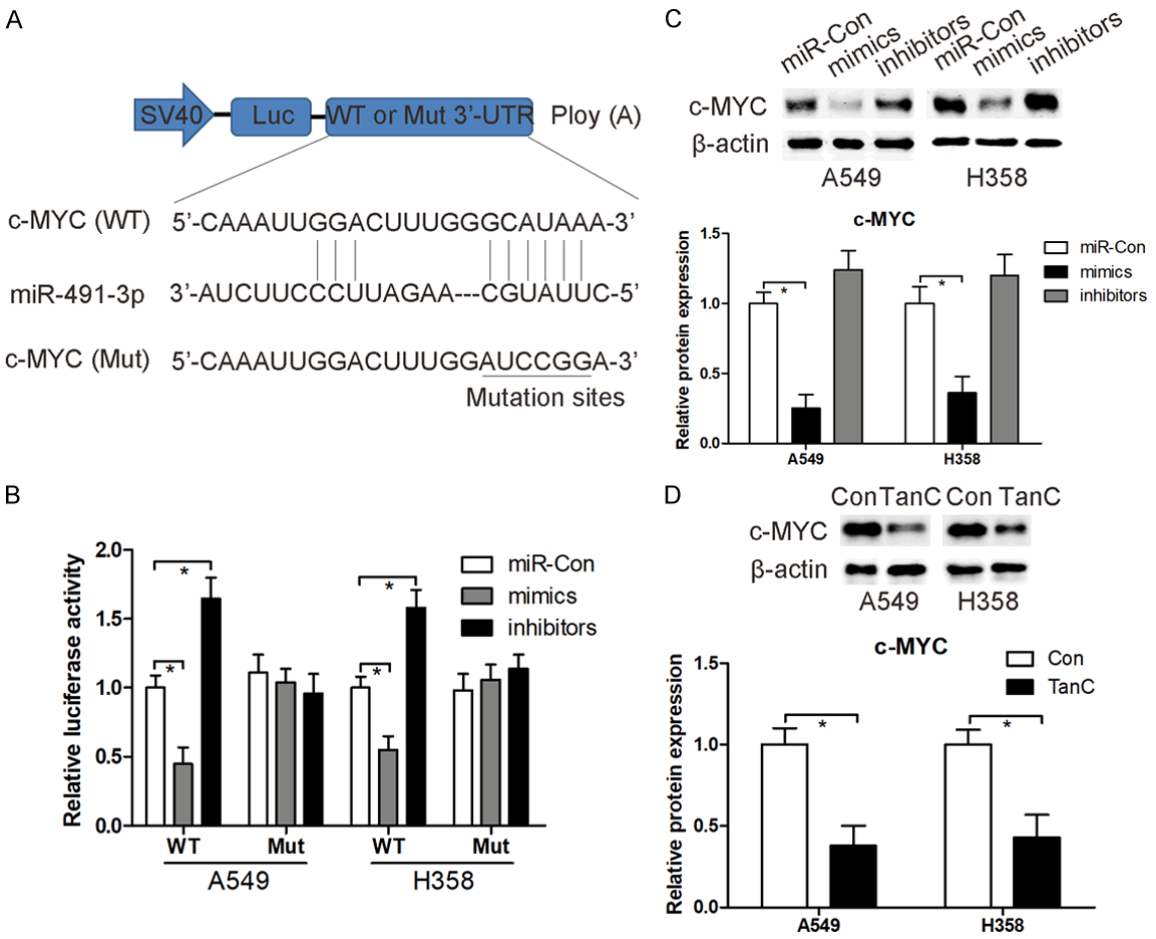

Figure 4. miR-491-3p negatively regulated c-MYC by directly binding to its 3'-UTR. Targetscan (A) and luciferase reporter assay (B) was conducted to confirm whether c-MYC was a direct target of miR-491-3p. After transfection with miR-Con, miR-491-3p mimics or inhibitors into A549 and H358 cells for 48 h, the protein expression levels of c-MYC were measured using western blotting (C). A549 and H358 cells exposure to TanC (10 μM) for 48 h, the protein expression levels of c-MYC were measured using western blotting (D). $^{*}P < 0.05$.

confirm whether the roles of miR-491-3p were depending on c-MYC in A549 and H358 cell proliferation and apoptosis, we conducted a rescue experiment. Both CCK8 (**Figure 5B**) and Annexinv-FITC double staining (**Figure 5C** and **5D**) assays discovered that miR-491-3p mimics induced growth inhibition and apoptosis were abolished by the overexpression of c-MYC in A549 and H358 cells.

Discussion

Recently, several studies point to expand multiple pharmacological functions and molecular mechanisms of TanC for human disease therapeutic applications [23, 24]. For instance, TanC is proposed as a potential anti-atherosclerotic agent via activating anti-oxidant peroxiredoxin 1/adenosine triphosphate-binding cassette transporter A1 signaling pathway, which contributes to inhibition of oxidized low-density lipoprotein induced macrophage foam cell formation [24]. In addition, TanC can serve as methyltransferase inhibitor and possesses an anticancer activity in various tumor cell lines, including lymphoma, prostate cancer, glioma and lung adenocarcinoma, through the inhibition of EZH2 activity [23].

In the present study, we further explored the antineoplastic activity and the underlying molecular mechanisms of TanC in NSCLC. Our findings revealed that TanC treatment led to a decrease in growth rate and an increase in apoptotic proportion of A549 and H358 cells, and the underlining mechanism was mediated,

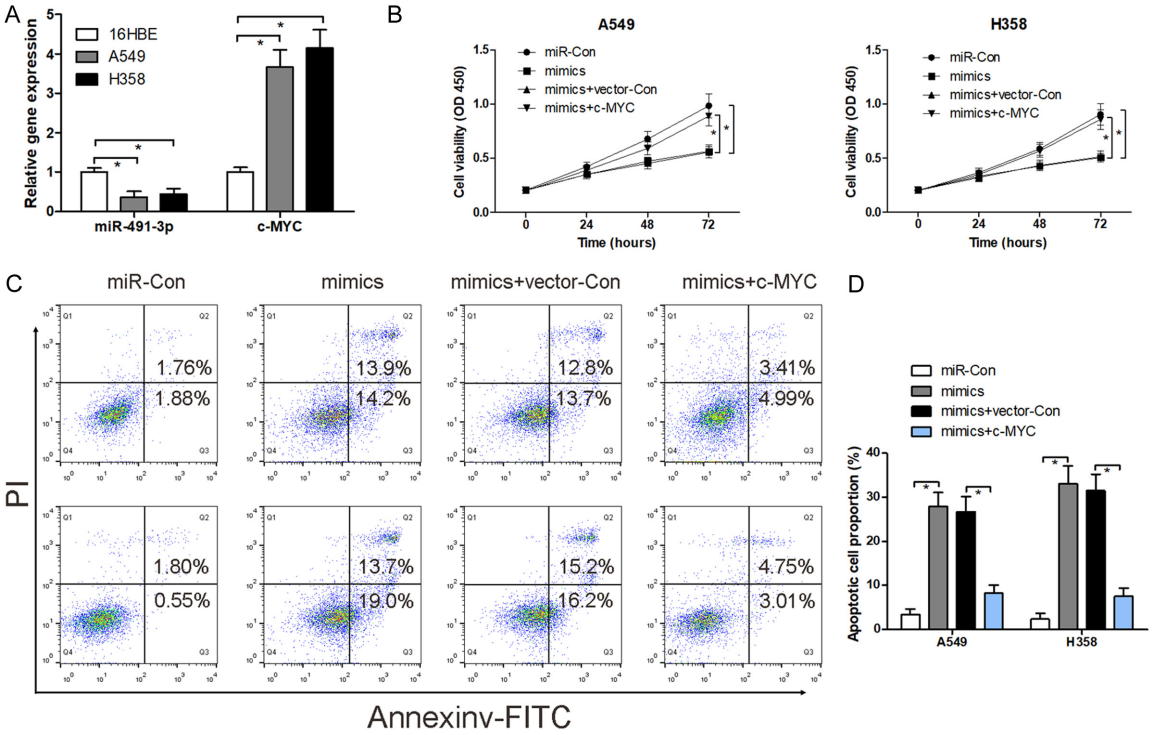

Figure 5. Overexpressed c-MYC rescued the miR-491-3p-mediated effects. The mRNA levels of miR-491-3p and c-MYC were measured using RT-qPCR (A). After co-transfection with c-MYC overexpressed plasmids and miR-491-3p mimics into A549 and H358 cells, cell viability (B) and apoptosis (C and D) were detected using CCK8 and Annexinv-FITC double staining, respectively. $^{*}P < 0.05$.

at least partially, by regulating miR-491-3p/c-MYC signaling pathway. Woo et al indicated that TanC represses growth of A549 cells with half maximal growth-inhibitory concentration of 4.2 ± 1.1 μM [23]. Consistent with this conclusion, our results showed that TanC significantly suppressed A549 cell proliferation when the concentration of TanC was more than 1 μM. Moreover, Woo et al also revealed that TanC can induce necrotic and apoptotic cell death in Pfeiffer cells [23].

On the other hand, miRNA microarray and RT-qPCR validated that TanC increased miR-491-3p expression in A549 and H358 cells. miR-491-3p, as a mature miRNA, is produced by miR-491 [25]. The biological function studies exhibited that miR-491-3p has been shown to inhibit proliferation, induce apoptosis and modulate chemo-sensitivity in different cancer types [25-27]. After transfection with miR-491-3p mimics into A549 and H358 cells, cell viability was found to be significantly reduced, and cell apoptotic rate was markedly elevated compared with the control group. These data suggested that miR-491-3p could function as a tumor suppressor in the tumorigenesis of NSCLC. This observation sparked our interest to investigate whether miR-491-3p mediated downstream target gene participates in these processes.

Notably, we found that c-MYC was a direct target of miR-491-3p, and overexpression of miR-491-3p repressed c-MYC protein expression by directly binding with the 3'-UTR of c-MYC. The transcription factor c-MYC, as an oncogene, has been reported to be associated with the initiation and progression of cancers [28] and is frequently found to be activated in various animal and human tumors [29, 30]. Although c-MYC has the ability to induce cell proliferation, pro-apoptotic function of c-MYC is discovered in cancer cells with high c-MYC levels, which may be associated with better treatment in response to anti-mitotic cancer therapeutics [31, 32]. These findings indicate that c-MYC may possess a peculiar dual role in the carcinogenesis. Miao et al shows that c-MYC mRNA and protein expression levels are higher in

NSCLC tissues and cell lines than those in the corresponding group [33]. Krysan et al demonstrated that an increase in c-MYC expression level is able to stimulate cell proliferation and promote resistance to pharmacologically induced apoptosis in NSCLC cells [34]. In our study, c-MYC was increased in A549 and H358 cells, and overexpression of c-MYC reversed the effect of miR-491-3p on NSCLC cell lines.

In conclusion, our study had identified that TanC possessed an effective ability to inhibit proliferation and induce apoptosis in NSCLC cells. More importantly, study on molecular mechanism reveals that miR-491-3p/c-MYC signaling pathway might be a novel therapeutic target of TanC for hindering the progression of NSCLC.

Disclosure of conflict of interest

None.

Address correspondence to: Dr. Bi-Yu Xu, Department of Traditional Chinese Medicine, The First Affiliated Hospital of Sun Yat-sen University, No. 58 Second Zhongshan Road, Guangzhou 510080, China. Tel: (+86)020-87755766-8387; Fax: (+86) 020-87755766-8387; E-mail: xubiyu@mail.sysu.edu.cn

References

[1] Torre LA, Bray F, Siegel RL, Ferlay J, Lortet-Tieulent J and Jemal A. Global cancer statistics, 2012. CA Cancer J Clin 2015; 65: 87-108.
[2] Chen W, Zheng R, Baade PD, Zhang S, Zeng H, Bray F, Jemal A, Yu XQ and He J. Cancer statistics in China, 2015. CA Cancer J Clin 2016; 66: 115-132.
[3] Siegel RL, Miller KD and Jemal A. Cancer statistics, 2018. CA Cancer J Clin 2018; 68: 7-30.
[4] Herbst RS, Morgensztern D and Boshoff C. The biology and management of non-small cell lung cancer. Nature 2018; 553: 446-454.
[5] Zhang J, Liang R, Wang L and Yang B. Effects and mechanisms of Danshen-Shanzha herb-pair for atherosclerosis treatment using network pharmacology and experimental pharmacology. J Ethnopharmacol 2019; 229: 104-114.
[6] Huang M, Wang P, Xu S, Xu W, Xu W, Chu K and Lu J. Biological activities of salvianolic acid B from Salvia miltiorrhiza on type 2 diabetes induced by high-fat diet and streptozotocin. Pharm Biol 2015; 53: 1058-1065.
[7] Gao D, Mendoza A, Lu S and Lawrence DA. Immunomodulatory effects of danshen (salvia miltiorrhiza) in BALB/c mice. ISRN Inflamm 2012; 2012: 954032.
[8] Yan Y, Su W, Zeng S, Qian L, Chen X, Wei J, Chen N, Gong Z and Xu Z. Effect and mechanism of tanshinone I on the radiosensitivity of lung cancer cells. Mol Pharm 2018; 15: 4843-4853.
[9] Ma S, Lei Y, Zhang L and Wang J. Research on the inhibiting effect of tanshinone IIA on colon cancer cell growth via COX-2-Wnt/beta-catenin signaling pathway. J BUON 2018; 23: 1337-1342.
[10] Sui H, Zhao J, Zhou L, Wen H, Deng W, Li C, Ji Q, Liu X, Feng Y, Chai N, Zhang Q, Cai J and Li Q. Tanshinone IIA inhibits beta-catenin/VEGF-mediated angiogenesis by targeting TGF-beta1 in normoxic and HIF-1alpha in hypoxic microenvironments in human colorectal cancer. Cancer Lett 2017; 403: 86-97.
[11] Tse AK, Chow KY, Cao HH, Cheng CY, Kwan HY, Yu H, Zhu GY, Wu YC, Fong WF and Yu ZL. The herbal compound cryptotanshinone restores sensitivity in cancer cells that are resistant to the tumor necrosis factor-related apoptosis-inducing ligand. J Biol Chem 2013; 288: 29923-29933.
[12] Yen JH, Huang HS, Chuang CJ and Huang ST. Activation of dynamin-related protein 1 - dependent mitochondria fragmentation and suppression of osteosarcoma by cryptotanshinone. J Exp Clin Cancer Res 2019; 38: 42.
[13] Sha W, Zhou Y, Ling ZQ, Xie G, Pang X, Wang P and Gu X. Antitumor properties of Salvianolic acid B against triple-negative and hormone receptor-positive breast cancer cells via ceramide-mediated apoptosis. Oncotarget 2018; 9: 36331-36343.
[14] Zheng X, Chen S, Yang Q, Cai J, Zhang W, You H, Xing J and Dong Y. Salvianolic acid A reverses the paclitaxel resistance and inhibits the migration and invasion abilities of human breast cancer cells by inactivating transgelin 2. Cancer Biol Ther 2015; 16: 1407-1414.
[15] Meister G. miRNAs get an early start on translational silencing. Cell 2007; 131: 25-28.
[16] Croce CM. Causes and consequences of microRNA dysregulation in cancer. Nat Rev Genet 2009; 10: 704-714.
[17] Cheng CJ, Bahal R, Babar IA, Pincus Z, Barrera F, Liu C, Svoronos A, Braddock DT, Glazer PM, Engelman DM, Saltzman WM and Slack FJ. MicroRNA silencing for cancer therapy targeted to the tumour microenvironment. Nature 2015; 518: 107-110.
[18] Jeon YJ, Kim T, Park D, Nuovo GJ, Rhee S, Joshi P, Lee BK, Jeong J, Suh SS, Grotzke JE, Kim SH, Song J, Sim H, Kim Y, Peng Y, Jeong Y, Garofalo M, Zanesi N, Kim J, Liang G, Nakano I, Cresswell P, Nana-Sinkam P, Cui R, Croce CM. miRNA-mediated TUSC3 deficiency enhances

UPR and ERAD to promote metastatic potential of NSCLC. Nat Commun 2018; 9: 5110.
[19] Garofalo M, Romano G, Di Leva G, Nuovo G, Jeon YJ, Ngankeu A, Sun J, Lovat F, Alder H, Condorelli G, Engelman JA, Ono M, Rho JK, Cascione L, Volinia S, Nephew KP and Croce CM. EGFR and MET receptor tyrosine kinase-altered microRNA expression induces tumorigenesis and gefitinib resistance in lung cancers. Nat Med 2011; 18: 74-82.
[20] Kim DH, Chang MS, Yoon CJ, Middeldorp JM, Martinez OM, Byeon SJ, Rha SY, Kim SH, Kim YS and Woo JH. Epstein-Barr virus BARF1-induced NFkappaB/miR-146a/SMAD4 alterations in stomach cancer cells. Oncotarget 2016; 7: 82213-82227.
[21] Livak KJ and Schmittgen TD. Analysis of relative gene expression data using real-time quantitative PCR and the 2(-Delta Delta C(T)) method. Methods 2001; 25: 402-408.
[22] Gong J, Wang ZX and Liu ZY. miRNA1271 inhibits cell proliferation in neuroglioma by targeting fibronectin 1. Mol Med Rep 2017; 16: 143-150.
[23] Woo J, Kim HY, Byun BJ, Chae CH, Lee JY, Ryu SY, Park WK, Cho H and Choi G. Biological evaluation of tanshindiols as EZH2 histone methyltransferase inhibitors. Bioorg Med Chem Lett 2014; 24: 2486-2492.
[24] Yang Y, Li X, Peng L, An L, Sun N, Hu X, Zhou P, Xu Y, Li P and Chen J. Tanshindiol C inhibits oxidized low-density lipoprotein induced macrophage foam cell formation via a peroxiredoxin 1 dependent pathway. Biochim Biophys Acta Mol Basis Dis 2018; 1864: 882-890.
[25] Li X, Liu Y, Granberg KJ, Wang Q, Moore LM, Ji P, Gumin J, Sulman EP, Calin GA, Haapasalo H, Nykter M, Shmulevich I, Fuller GN, Lang FF and Zhang W. Two mature products of MIR-491 coordinate to suppress key cancer hallmarks in glioblastoma. Oncogene 2015; 34: 1619-1628.
[26] Zheng G, Jia X, Peng C, Deng Y, Yin J, Zhang Z, Li N, Deng M, Liu X, Liu H, Lu M, Wang C, Gu Y and He Z. The miR-491-3p/mTORC2/FOXO1 regulatory loop modulates chemo-sensitivity in human tongue cancer. Oncotarget 2015; 6: 6931-6943.
[27] Zhao Y, Qi X, Chen J, Wei W, Yu C, Yan H, Pu M, Li Y, Miao L, Li C and Ren J. The miR-491-3p/Sp3/ABCB1 axis attenuates multidrug resistance of hepatocellular carcinoma. Cancer Lett 2017; 408: 102-111.
[28] Adhikary S and Eilers M. Transcriptional regulation and transformation by Myc proteins. Nat Rev Mol Cell Biol 2005; 6: 635-645.
[29] Sun J, Cai X, Yung MM, Zhou W, Li J, Zhang Y, Li Z, Liu SS, Cheung ANY, Ngan HYS, Li Y, Dai Z, Kai Y, Tzatsos A, Peng W, Chan DW and Zhu W. miR-137 mediates the functional link between c-Myc and EZH2 that regulates cisplatin resistance in ovarian cancer. Oncogene 2019; 38: 564-580.
[30] Li M, Liu Y, Wei Y, Wu C, Meng H, Niu W, Zhou Y, Wang H, Wen Q, Fan S, Li Z, Li X, Zhou J, Cao K, Xiong W, Zeng Z, Li X, Qiu Y, Li G and Zhou M. Zinc-finger protein YY1 suppresses tumor growth of human nasopharyngeal carcinoma by inactivating c-Myc-mediated microRNA-141 transcription. J Biol Chem 2019; 294: 6172-6187.
[31] Topham C, Tighe A, Ly P, Bennett A, Sloss O, Nelson L, Ridgway RA, Huels D, Littler S, Schandl C, Sun Y, Bechi B, Procter DJ, Sansom OJ, Cleveland DW and Taylor SS. MYC is a major determinant of mitotic cell fate. Cancer Cell 2015; 28: 129-140.
[32] Aakko S, Straume AH, Birkeland EE, Chen P, Qiao X, Lonning PE and Kallio MJ. MYC-induced miR-203b-3p and miR-203a-3p control Bcl-xL expression and paclitaxel sensitivity in tumor cells. Transl Oncol 2019; 12: 170-179.
[33] Miao LJ, Huang SF, Sun ZT, Gao ZY, Zhang RX, Liu Y and Wang J. MiR-449c targets c-Myc and inhibits NSCLC cell progression. FEBS Lett 2013; 587: 1359-1365.
[34] Krysan K, Kusko R, Grogan T, O'Hearn J, Reckamp KL, Walser TC, Garon EB, Lenburg ME, Sharma S, Spira AE, Elashoff D and Dubinett SM. PGE2-driven expression of c-Myc and oncomiR-17-92 contributes to apoptosis resistance in NSCLC. Mol Cancer Res 2014; 12: 765-774.